

DTIC FILE COPY

4

NSWC TR 88-76

AD-A205 756

**INVESTIGATION OF Li/SO₂ CELL HAZARDS,
III. RAMAN SPECTROSCOPY OF LITHIUM
DITHIONITE**

BY W. P. KILROY (NSWC), AND
S. A. CHMIELEWSKI AND D. W. BENNETT (UNIVERSITY OF WISCONSIN)

RESEARCH AND TECHNOLOGY DEPARTMENT

1 SEPTEMBER 1988

Approved for public release; distribution is unlimited.

DTIC
ELECTE
MAR 10 1989
S & H D



NAVAL SURFACE WARFARE CENTER

Dahlgren, Virginia 22448-5000 • Silver Spring, Maryland 20903-5000

89 3 09 085

UNCLASSIFIED

SECURITY CLASSIFICATION OF THIS PAGE

REPORT DOCUMENTATION PAGE

1a REPORT SECURITY CLASSIFICATION UNCLASSIFIED			1b RESTRICTIVE MARKINGS	
2a SECURITY CLASSIFICATION AUTHORITY			3 DISTRIBUTION AVAILABILITY OF REPORT Approved for public release; distribution is unlimited.	
2b DECLASSIFICATION/DOWNGRADING SCHEDULE				
4 PERFORMING ORGANIZATION REPORT NUMBER(S) NSWC TR 88-76			5 MONITORING ORGANIZATION REPORT NUMBER(S)	
6a NAME OF PERFORMING ORGANIZATION Naval Surface Warfare Center		6b OFFICE SYMBOL (If applicable) Code R33		7a NAME OF MONITORING ORGANIZATION
6c ADDRESS (City, State, and ZIP Code) 10901 New Hampshire Avenue Silver Spring, MD 20903-5000			7b ADDRESS (City, State, and ZIP Code)	
8a NAME OF FUNDING SPONSORING ORGANIZATION Office of Naval Technology		8b OFFICE SYMBOL (If applicable)		9 PROCUREMENT INSTRUMENT IDENTIFICATION NUMBER
8c ADDRESS (City, State, and ZIP Code) 800 North Quincy Street Arlington, VA 22217			10 SOURCE OF FUNDING NUMBERS	
			PROGRAM ELEMENT NO	PROJECT NO
			TASK NO	WORK UNIT ACCESSION NO
11 TITLE (Include Security Classification) Investigation of Li/SO ₂ Cell Hazards, III. Raman Spectroscopy of Lithium Dithionite				
12 PERSONAL AUTHOR(S) Kilroy, W. P. (NSWC); Chmielewski, S. A.; and Bennett, D. W. (University of Wisconsin)				
13a TYPE OF REPORT	13b TIME COVERED FROM 6/85 TO 1/86		14 DATE OF REPORT (Year, Month, Day) 1988, September 1	15 PAGE COUNT 42
16 SUPPLEMENTARY NOTATION				
17 COSATI CODES			18 SUBJECT TERMS (Continue on reverse if necessary and identify by block number) Raman Spectroscopy Lithium Dithionite Sulfur Dioxide Battery, 7001-1	
FIELD	GROUP	SUB-GROUP		
07	04			
19 ABSTRACT (Continue on reverse if necessary and identify by block number) The preparation of pure lithium dithionite was investigated using several synthetic methods. Raman spectroscopy reveals that lithium dithionite undergoes a low-temperature lattice transformation that demonstrates the existence of two forms of dithionite. Transition metal ions were briefly evaluated as a first step in altering the SO ₂ reduction mechanism or for stabilizing dithionite.				
20 DISTRIBUTION/AVAILABILITY OF ABSTRACT <input type="checkbox"/> UNCLASSIFIED/UNLIMITED <input checked="" type="checkbox"/> SAME AS RPT <input type="checkbox"/> DTIC USERS			21 ABSTRACT SECURITY CLASSIFICATION UNCLASSIFIED	
22a NAME OF RESPONSIBLE INDIVIDUAL William P. Kilroy			22b TELEPHONE (Include Area Code) (202) 394-1513	22c OFFICE SYMBOL Code R33

DD FORM 1473, 84 MAR

83 APR edition may be used until exhausted

All other editions are obsolete

SECURITY CLASSIFICATION OF THIS PAGE

★ U.S. Government Printing Office: 1985-539-012

0102-LF-014-6602

i/ii

UNCLASSIFIED

CONTENTS

<u>Chapter</u>		<u>Page</u>
1	INTRODUCTION	1
2	SYNTHESIS OF LITHIUM DITHIONITE	3
	AQUEOUS PREPARATION	3
	NONAQUEOUS PREPARATIONS	4
3	SPECTROSCOPIC INVESTIGATIONS OF LITHIUM DITHIONITE . .	7
4	INVESTIGATION OF DITHIONITE STABILIZATION	27
5	SUMMARY	31
	REFERENCES	33
	DISTRIBUTION	(1)

ILLUSTRATIONS

<u>Figure</u>		<u>Page</u>
1	RAMAN SPECTRUM FOR SODIUM METABISULFITE	8
2	RAMAN SPECTRUM OF SODIUM THIOSULFATE	8
3	RAMAN SPECTRUM FOR SODIUM DITHIONATE DIHYDRATE	9
4	RAMAN SPECTRUM FOR SODIUM SULFITE	9
5	RAMAN SPECTRUM FOR SODIUM SULFATE	10
6	RAMAN SPECTRUM FOR SULFUR (S_2)	10
7	RAMAN SPECTRUM FOR LITHIUM DITHIONITE PREPARED IN AN AQUEOUS ENVIRONMENT	11
8	RAMAN SPECTRUM FOR LITHIUM DITHIONITE PREPARED BY A SCALED-UP NONAQUEOUS SELECTRIDE METHOD	11
9	RAMAN SPECTRUM FOR LITHIUM DITHIONITE PREPARED IN A NONAQUEOUS ENVIRONMENT	12
10	RAMAN SPECTRUM FOR LITHIUM DITHIONITE PREPARED IN A NONAQUEOUS ENVIRONMENT AFTER 35 WEEKS STORAGE SEALED UNDER N_2	12
11	ESR SPECTRA FOR NONAQUEOUS $Li_2S_2O_4$ AT AMBIENT TEMPERATURE: (a) ORIGINAL; (b) AFTER HEATING 4 MIN AT $135^\circ C$; (c) AFTER HEATING ADDITIONAL 2 MIN (TOTAL OF 6) AT $135^\circ C$	15

ILLUSTRATIONS (Cont.)

<u>Figure</u>		<u>Page</u>
12	DSC CURVE AT 20°C/MIN FOR LITHIUM DITHIONITE PREPARED IN AQUEOUS MEDIUM	16
13	DSC CURVE AT 20°C/MIN FOR LITHIUM DITHIONITE PREPARED IN NONAQUEOUS MEDIUM	17
14	RAMAN SPECTRUM FOR $\text{Li}_2\text{S}_2\text{O}_4$ (AQUEOUS PREPARATION) 15 MIN AT 160°C	18
15	RAMAN SPECTRUM FOR $\text{Li}_2\text{S}_2\text{O}_4$ (AQUEOUS PREPARATION) 60 MIN AT 160°C	19
16	RAMAN SPECTRUM FOR $\text{Li}_2\text{S}_2\text{O}_4$ (AQUEOUS PREPARATION) 150 MIN AT 160°C	20
17	RAMAN SPECTRUM FOR $\text{Li}_2\text{S}_2\text{O}_4$ (AQUEOUS PREPARATION) 360 MIN AT 160°C	21
18	RAMAN SPECTRUM FOR $\text{Li}_2\text{S}_2\text{O}_4$ (NONAQUEOUS PREPARATION) 10 MIN AT 160°C	22
19	RAMAN SPECTRUM FOR $\text{Li}_2\text{S}_2\text{O}_4$ (NONAQUEOUS PREPARATION) 20 MIN AT 160°C	23
20	RAMAN SPECTRUM FOR $\text{Li}_2\text{S}_2\text{O}_4$ (NONAQUEOUS PREPARATION) 60 MIN AT 160°C	24
21	RAMAN SPECTRUM OF SAMPLE DECOMPOSED AT 160°C FOR 20 MIN (FIGURE 19), THEN REGROUND AND RESCANNED	26
22	RAMAN SPECTRUM OF ZINC DITHIONITE	29
23	RAMAN SPECTRUM OF ZINC DITHIONITE PYRIDINE	30

CHAPTER 1

INTRODUCTION

The U.S. Navy requires high energy, portable power sources for many weapons applications. A high energy density power source is the Li/SO_2 system, which is a hazard to military personnel under adverse and misuse conditions such as high drain rates, forced overdischarge, and charging.

Despite many studies, it remains difficult to define one mechanism that explains all hazardous events. Although lithium dithionite is the product formed when the Li/SO_2 cell is discharged under low rate ambient conditions, a complex array of chemicals is produced when the cell is used under other modes of operation, e.g., use-storage-reuse, pulsing, nonambient discharge, etc. This problem is compounded by the use of different cell balances and cell designs. Even the concentrations of impurities present, such as water, change from day to day.

The principal mechanism of safety hazards occurring in SO_2 cells appears to involve the thermal decomposition of lithium dithionite and subsequent reactions during high rate discharge or overdischarge.¹ Since dithionite is the initial product and is central to the mechanism for safety hazards, the objectives of this study were twofold: (1) to examine the stability of dithionite by Raman spectroscopy to probe further into the chemical decomposition, and (2) to begin to improve the safety by either altering the discharge mechanism and/or by improving the thermal stability of dithionite.

CHAPTER 2

SYNTHESIS OF LITHIUM DITHIONITE

Since lithium dithionite is not commercially available and very difficult to prepare, much effort was expended in attempts to synthesize pure material. Summarized below are the experimental details of the various reactions attempted. The unsuccessful or marginally successful reactions are treated with brevity. All of the reactions employed SO_2 as a reactant.

AQUEOUS PREPARATION

Lithium dithionite was synthesized by adding solutions of water, lithium hydroxide, lithium formate and sulfur dioxide in methanol, and methyl formate into a reactor containing methanol.

The reaction vessel was constructed of glass and type 316 stainless steel, with a cold finger heat exchanger for cooling and heating, a reflux condenser, a pressure regulator, and a thermocouple connected to a digital temperature readout.

The solutions were fed into the reactor over a 60-minute period, maintaining a temperature of 65°C and a pressure of 20 psig. The material was allowed to cook for 2 hours after the additions, until CO_2 ceased to evolve.

The reaction mass was then cooled, vacuum filtered under an inert gas, transferred to a glass container, and vacuum dried in a hot water bath. The product was light tan in color and was obtained in 67% yield. It was analyzed as 90.8% lithium dithionite.

NONAQUEOUS PREPARATIONS

LITHIUM

Ammonia was condensed over elemental lithium in a vacuum line. While the ammoniated lithium was being stirred, it was exposed to gaseous sulfur dioxide at -30°C . A white solid mixture containing sulfur, oxygen, and nitrogen with no simple stoichiometry was formed. Assay with methylene blue revealed less than 3% dithionite.

 LiAlH_4

SO_2 was condensed into an ether solution of LiAlH_4 in a vacuum line. A white solid formed when the reaction mixture was allowed to warm to room temperature. The solid was insoluble in water and did not reduce methylene blue.

Lithium Naphtholide

Lithium naphtholide was too powerful a reducing agent, giving rise to sulfur and lithium sulfide.

Lithium Benzophenone Ketyl

Bowden, et al. describe the use of this reagent in THF.² They report a 70% yield based on a rather equivocal UV spectroscopic assay. We attempted the same reaction but were unable to produce a satisfactory product. Titration with methylene blue indicated the solid was 27% $\text{Li}_2\text{S}_2\text{O}_4$.

LiBH₄

Since over-reduction appeared to be a problem in the above reactions, we attempted to improve the yield of dithionite by using a weaker reducing agent, LiBH₄. Fifty ml of degassed THF containing 1.2 g SO₂ was added to a stirred solution of 1 mmole LiBH₄ in 200 ml degassed THF over a 5 minute period. The white product was washed with anhydrous oxygen-free methanol under nitrogen. Titration with methylene blue indicated the solid contained 23% dithionite.

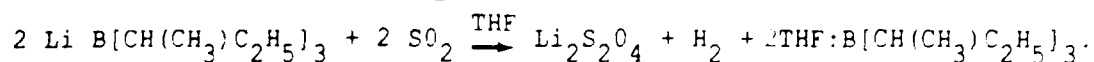
L-Selectride

Alkali metal selectrides are known to be milder reducing agents than either sodium borohydride or lithium aluminum hydride. L-Selectride (LiB[CH(CH₃)C₂H₅]₃H), an Aldrich product, proved to be the most promising reagent for the non-aqueous synthesis of Li₂S₂O₄. The initial reaction was run at room temperature, providing a product containing 44% lithium dithionite. Raman spectra indicated that sulfur-oxy anions were the major impurities, and that over-reduction was not a factor in this process. To slow down oxygen atom transfer and subsequent formation of thiosulfate, metabisulfite, etc., we repeated the reaction at a low temperature as described below.

A 250 ml Schlenk flask fitted with a rubber septum was purged with dry nitrogen. Then, 125 ml of dry degassed THF was added via syringe; 13.4 mmoles of SO₂ were added through an inlet needle (determined by weighing the flask and contents). The flask was immersed in an isopropanol-dry ice bath until the flask temperature equilibrated at -78°C. Nitrogen was added until the flask pressure was approximately one atmosphere. Then 13 ml of 1M L-Selectride (13.0 mmoles) was added slowly via syringe. The N₂ purge was removed since the selectride reacted

immediately and the reaction was monitored via the H_2 gas exiting an outlet stopcock into oil. The solution was stirred for 1 hour at $-78^\circ C$. The solution and white product were allowed to warm to room temperature and were filtered using a 10-20 micron Schlenk frit. The product was thoroughly washed three times with dry THF followed by a final wash with dry ether. Thorough washing with THF was required to react the butylborohydride to form the acid-base adduct; otherwise, any residual $B[CH(CH_3)C_2H_5]_3$ might have burned in an open container or exploded in a closed container upon exposure or admission of air or water. The product was dried in vacuo, gently ground in an inert glove bag, and assayed by titration with methylene blue.³ The preparations assayed between 82-92% dithionite. Raman spectroscopy revealed only dithionite vibrations.

A 10 fold excess of THF to selectride should be used to get good reproducible results. The solvent dependency is probably related to kinetic formation of the $THF:B[CH(CH_3)C_2H_5]_3$ acid-base adduct. The reaction of lithium tri-sec-butylborohydride and SO_2 can be written:



CHAPTER 3
SPECTROSCOPIC INVESTIGATIONS OF LITHIUM DITHIONITE

A major factor contributing to Li/SO₂ cell hazards appears to be the thermal decomposition of lithium dithionite and subsequent reactions. Depending on cell conditions, a number of decomposition pathways are possible.^{2,4} Raman spectroscopy was selected as the method of choice to investigate the decomposition mechanism. Raman spectra of various solid salts, shown in Figures 1 through 6, exhibit discernible vibrational bands in the 150-600 cm⁻¹ region.

In an effort to scale up the non-aqueous synthesis of Li₂S₂O₄ to provide larger samples for future accelerating rate calorimetry (ARC) studies, we inadvertently produced a sample of lithium dithionite which was remarkably unstable with respect to solid state oxidation. In attempting to weigh the material on an analytical balance (in air), the material decomposed spontaneously and exothermically on the balance. Since the material is made from lithium selectride, we initially concluded that some residual borohydride material remained on the solid, and had initiated the thermal decomposition of the lithium dithionite upon contact with the air. Therefore, we thoroughly washed a portion of the sample with THF, in which all the possible borohydride materials are extremely soluble. Exposure of the washed material to air resulted in the same facile decomposition.

Capillary tubes filled with lithium dithionite were sealed under nitrogen and Raman spectra recorded. The data in Figures 7 through 9 reveal interesting differences in the low-frequency band. Figure 7 shows a symmetrical peak at 281 cm⁻¹ for dithionite prepared by the aqueous synthesis. Raman data for

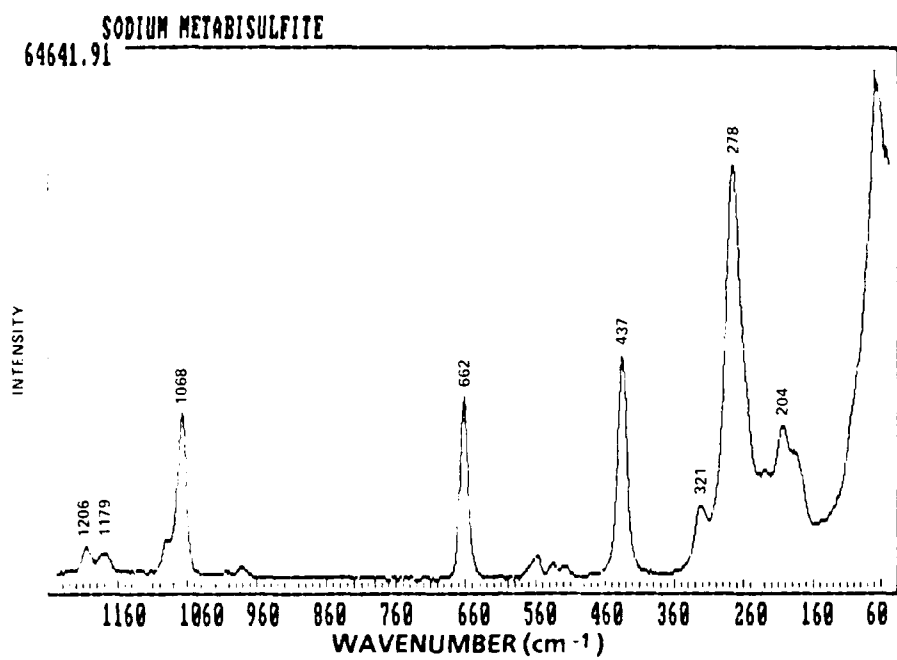


FIGURE 1. RAMAN SPECTRUM FOR SODIUM METABISULFITE

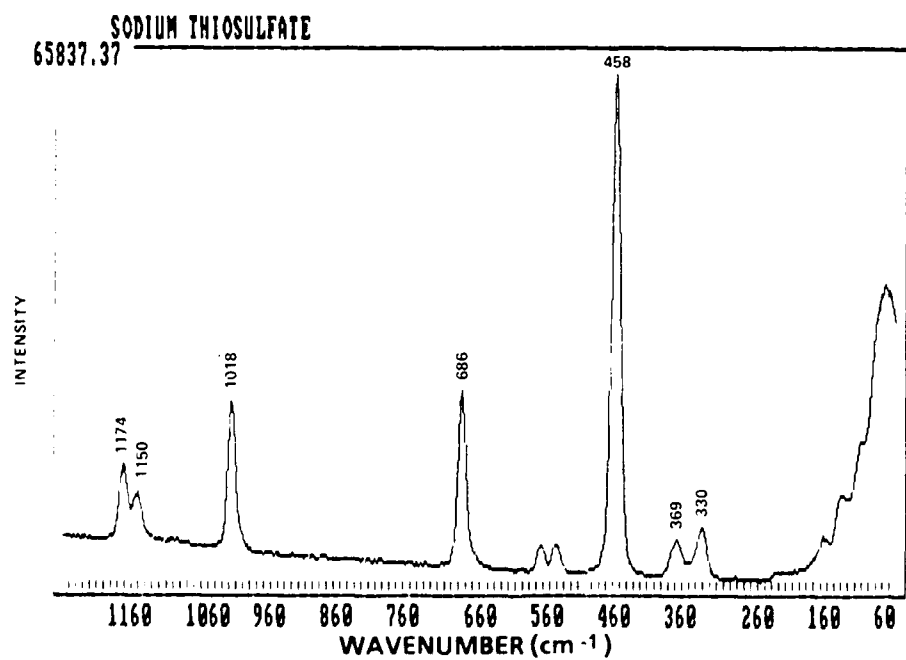


FIGURE 2. RAMAN SPECTRUM OF SODIUM THIOSULFATE

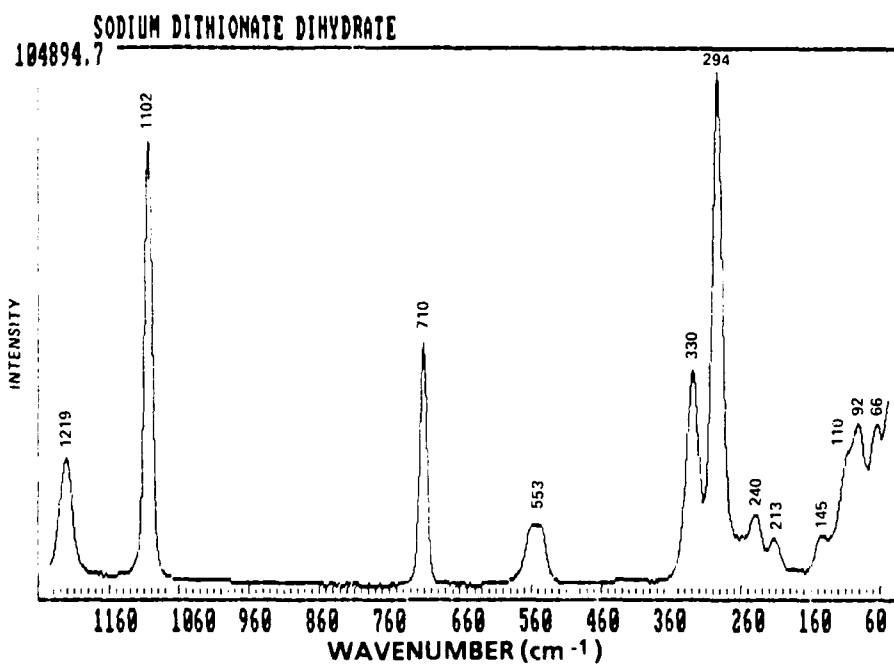


FIGURE 3. RAMAN SPECTRUM FOR SODIUM DITHIONATE DIHYDRATE

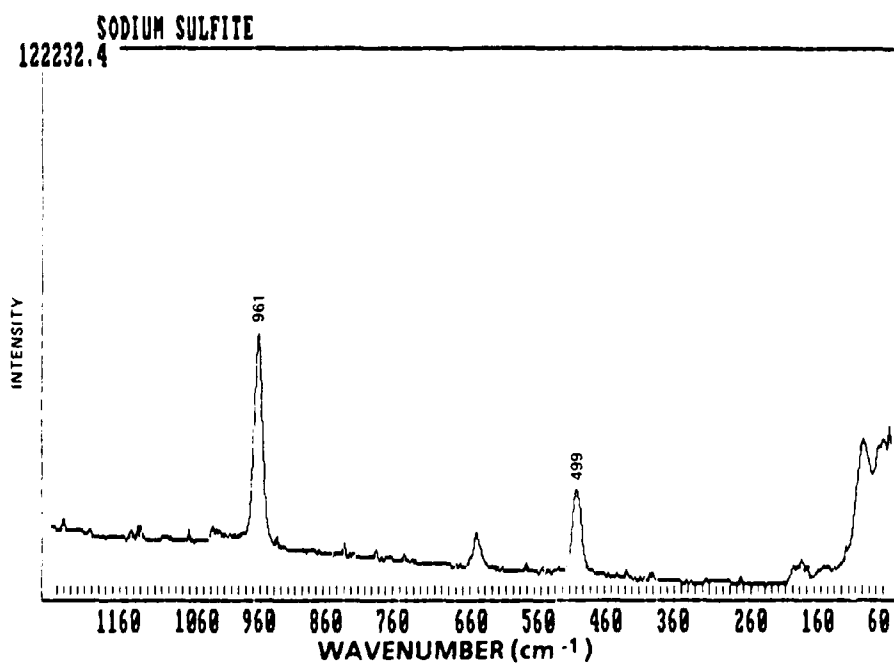


FIGURE 4. RAMAN SPECTRUM FOR SODIUM SULFITE

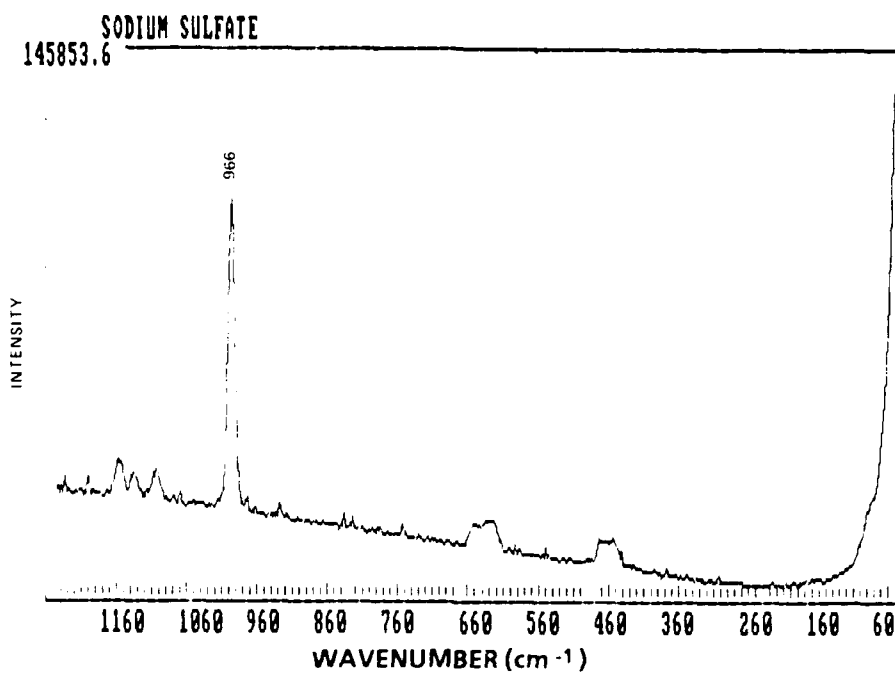
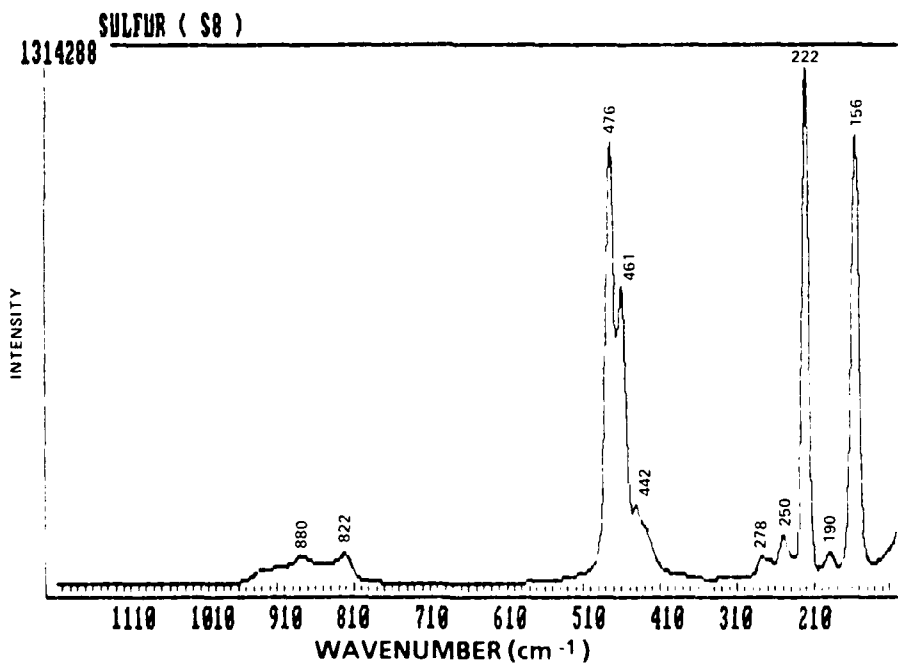


FIGURE 5. RAMAN SPECTRUM FOR SODIUM SULFATE

FIGURE 6. RAMAN SPECTRUM FOR SULFUR (S₂)

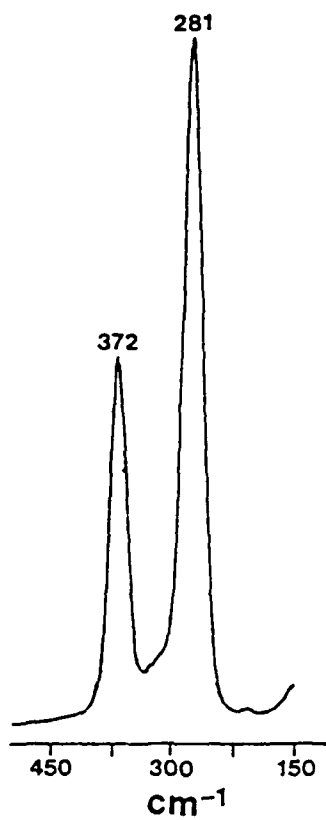


FIGURE 7. RAMAN SPECTRUM FOR LITHIUM DITHIONITE PREPARED IN AN AQUEOUS ENVIRONMENT

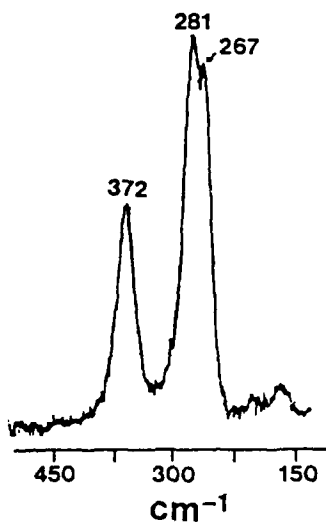


FIGURE 8. RAMAN SPECTRUM FOR LITHIUM DITHIONITE PREPARED BY A SCALED-UP NONAQUEOUS SELECTRIDE METHOD

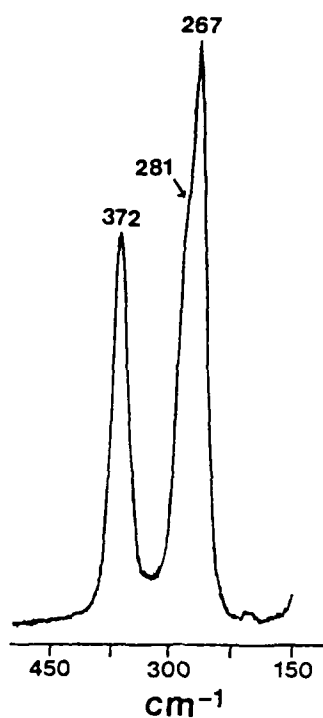


FIGURE 9. RAMAN SPECTRUM FOR LITHIUM DITHIONITE PREPARED IN A NONAQUEOUS ENVIRONMENT

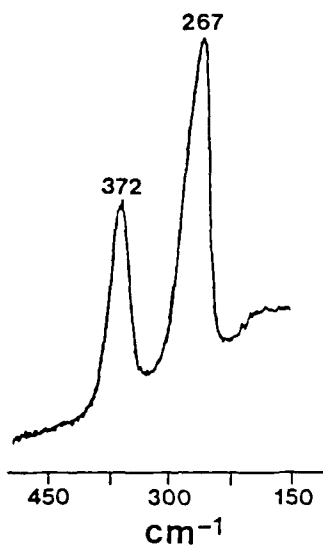


FIGURE 10. RAMAN SPECTRUM FOR LITHIUM DITHIONITE PREPARED IN A NONAQUEOUS ENVIRONMENT AFTER 35 WEEKS STORAGE SEALED UNDER N₂

dithionite prepared by the scaled-up (but otherwise identical) selectride process are shown in Figure 8. The major peak occurs at 281 cm^{-1} and a second band appears at 267 cm^{-1} . The Raman spectrum for dithionite prepared by the small scale selectride method described is shown in Figure 9. Now the major band occurs at 267 cm^{-1} with a small shoulder at 281 cm^{-1} .

Raman peaks for the dithionite anion are unmistakable due to their intensity in the solid state. The proximity of the 281 cm^{-1} frequencies suggest they are due to two different S-S stretching frequencies in the extremely polarizable $\text{S}_2\text{O}_4^{2-}$ anion. This indicates the anion exists in two different environments, and may explain the various susceptibilities to oxidation and thermal stability. The stability of the dithionite may be related to a low-temperature lattice transformation. When the initial sample of $\text{Li}_2\text{S}_2\text{O}_4$ exhibiting both peaks was heated at 60°C under vacuum for 1 hour, the two low-frequency peaks merged into a single sharp peak at 281 cm^{-1} , as occurs with a recrystallized sample.

When the nonaqueous sample of $\text{Li}_2\text{S}_2\text{O}_4$ was dissolved in basic aqueous solution and lyophilized, the 267 cm^{-1} peak disappeared, leaving a spectrum identical to the material obtained in an aqueous environment. In contrast, Figure 10 shows a spectrum of the nonaqueous sample of $\text{Li}_2\text{S}_2\text{O}_4$ after the material was stored for 35 weeks in a sealed capillary tube in which the peak at 281 cm^{-1} was significantly diminished. This indicates a conversion to the "new" form of lithium dithionite in the solid state. This apparent tendency for lattice transformation at remarkably low temperatures could be important in the solid state decomposition process, since lattice motion is often requisite for the formation of lattice defect sites and the propagation of solid state reactions. It is equally important to point out here that the type of lithium dithionite formed under nonaqueous conditions is not observed after the material is recrystallized from aqueous solution.

The two resonance bands present in the ESR spectra of $\text{Li}_2\text{S}_2\text{O}_4$ (Figure 11) indicate existence of the sulfoxylate radical in two environments. A low-temperature transformation is evidenced by the decrease in intensity of the bands as the sample is heated. The radical anion concentration never increases with increasing temperature of the dithionite. This calls to question the general premise that the radical anion is involved in the decomposition process.

The thermal decomposition of lithium dithionite was investigated using DSC and Raman spectroscopy. The DSC thermal stability of the dithionites prepared by the aqueous and nonaqueous methods are compared at a heating rate of $20^\circ\text{C}/\text{min}$ in Figures 12 and 13, respectively. The sample prepared in a nonaqueous medium was less stable, decomposing $\sim 32^\circ$ lower than the "aqueous" dithionite.

Raman spectroscopy was also employed since it was originally thought this method would give insight into the decomposition process. In addition to the Raman data in Figures 1 through 6, Raman bands for tri-, tetra-, and penta- thionates were reported at 425, 390, and 392 cm^{-1} , respectively.⁵ As it turned out, the S-S stretching bands of the dithionite and elemental sulfur were much more intense than the other oxy-sulfur anions, making it difficult to identify various products during the decomposition.

Dithionite samples, sealed in capillary tubes, were heated in a temperature-controlled oil bath. The samples were quenched at the desired temperature and Raman data recorded at room temperature.

Raman data for the dithionite prepared by the aqueous method are shown in Figures 14 through 17. The decomposition temperature for this material, defined by our somewhat arbitrary criteria, was found to be near 160°C . Even after 150 minutes, the material was far from totally decomposed. Essentially complete decomposition was observed after six hours. In contrast, Raman data for the dithionite prepared in nonaqueous medium, shown in Figures 18 through 20, reveal decomposition progressed much more rapidly at this temperature.

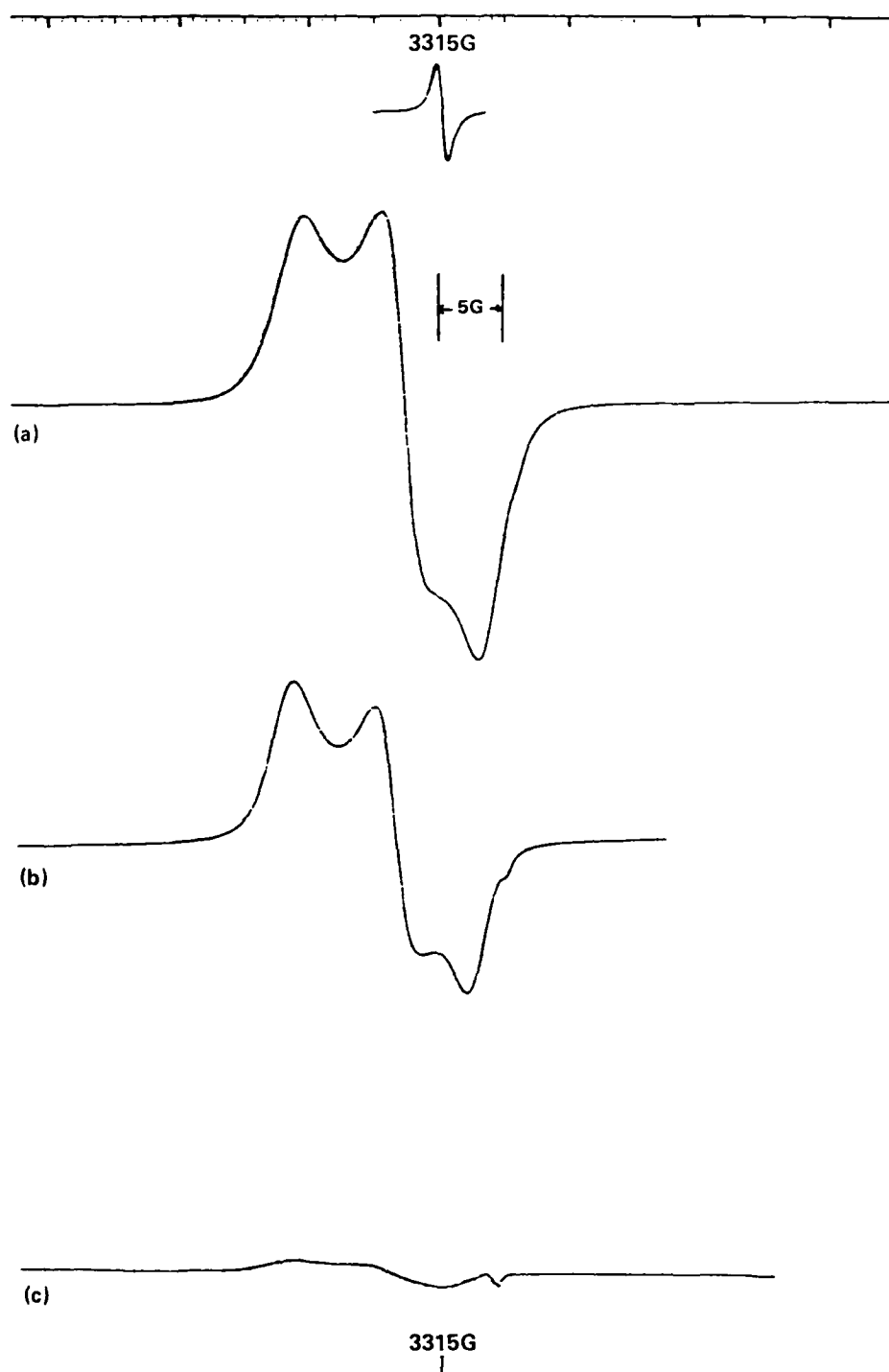


FIGURE 11. ESR SPECTRA FOR NONAQUEOUS $\text{Li}_2\text{S}_2\text{O}_4$ AT AMBIENT TEMPERATURE: (a) ORIGINAL; (b) AFTER HEATING 4 MIN AT 135°C ; (c) AFTER HEATING ADDITIONAL 2 MIN (TOTAL OF 6) AT 135°C

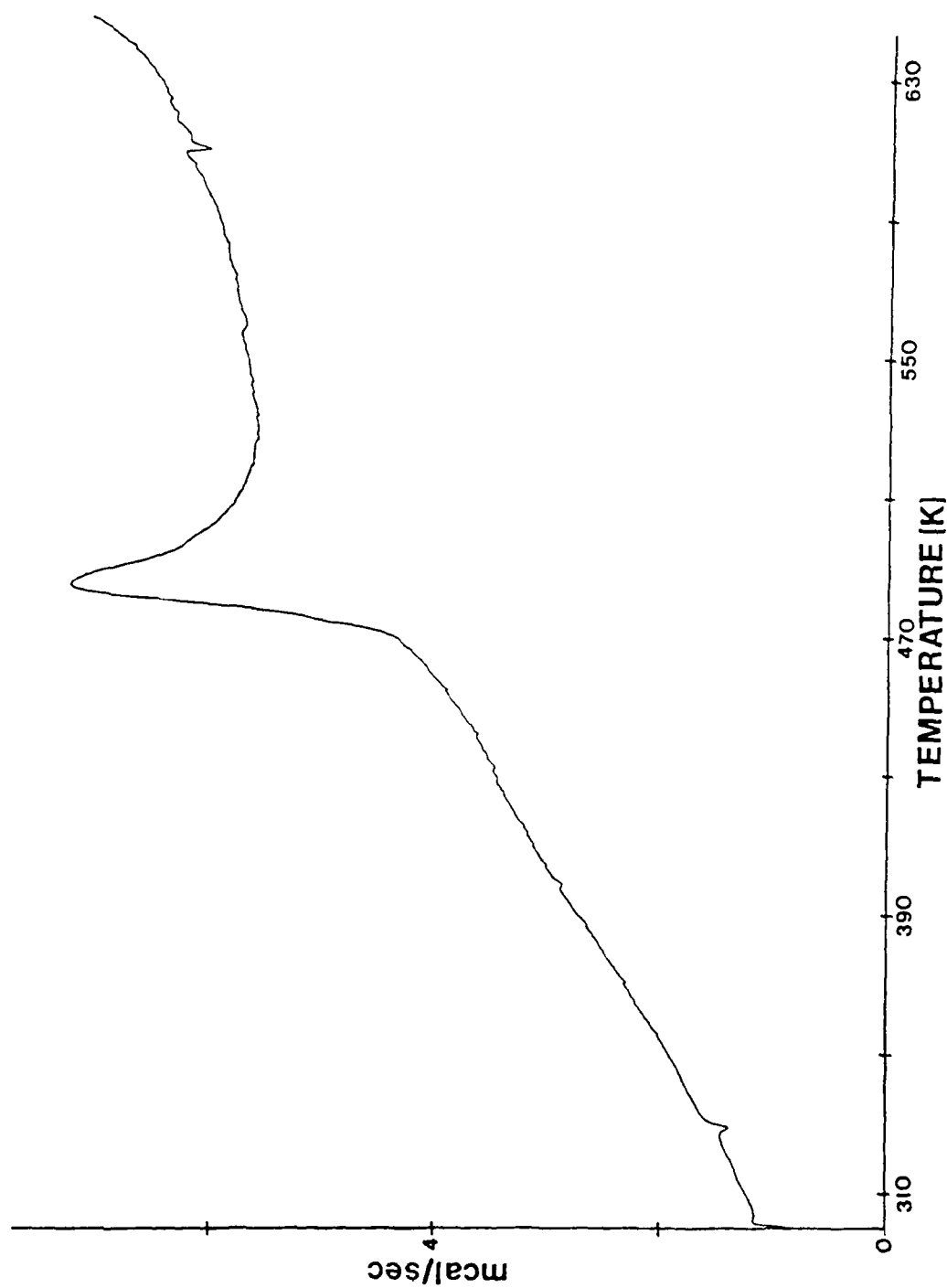


FIGURE 12. DSC CURVE AT 20°C/MIN FOR LITHIUM DITHIONITE PREPARED IN AQUEOUS MEDIUM

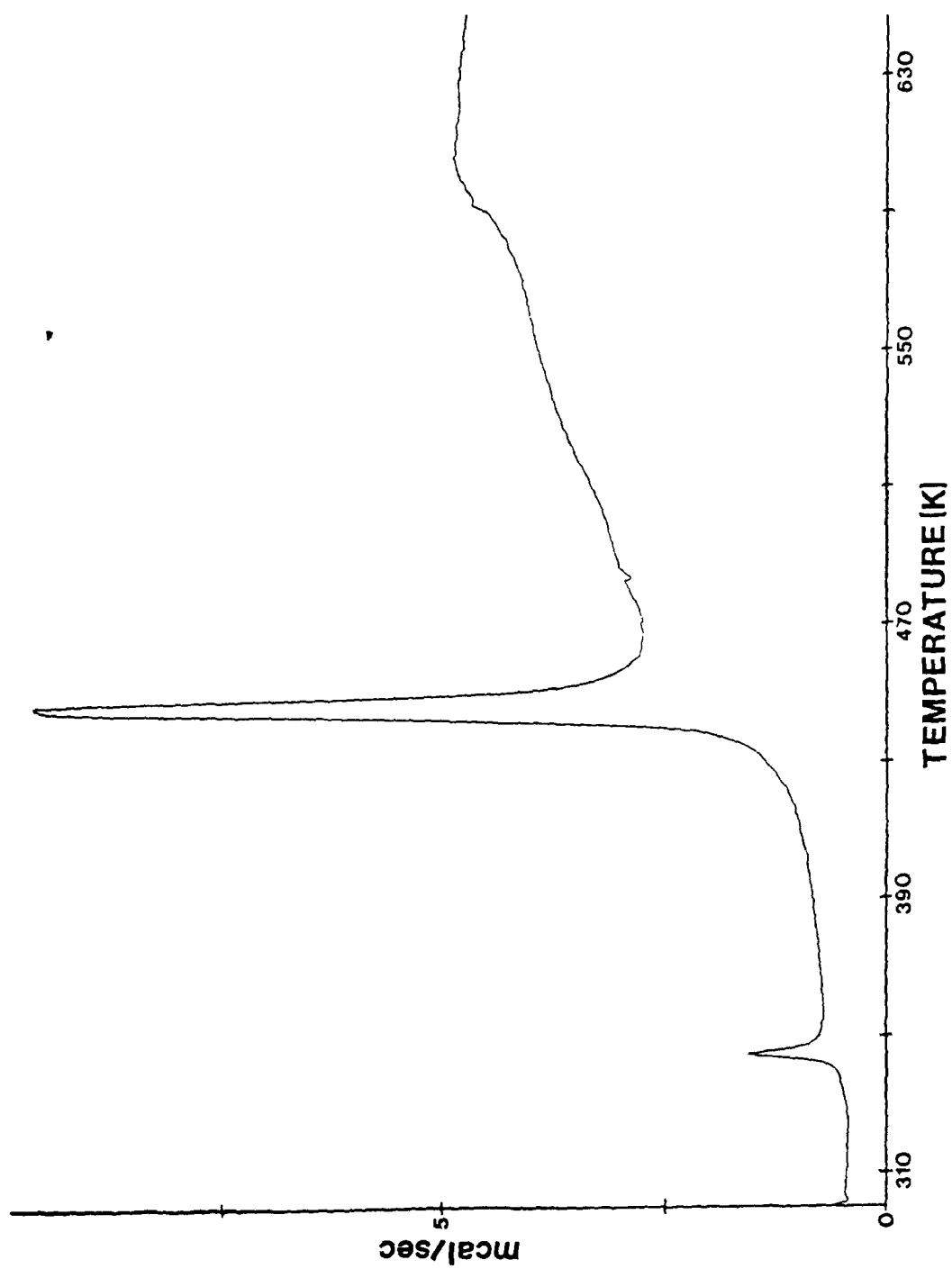
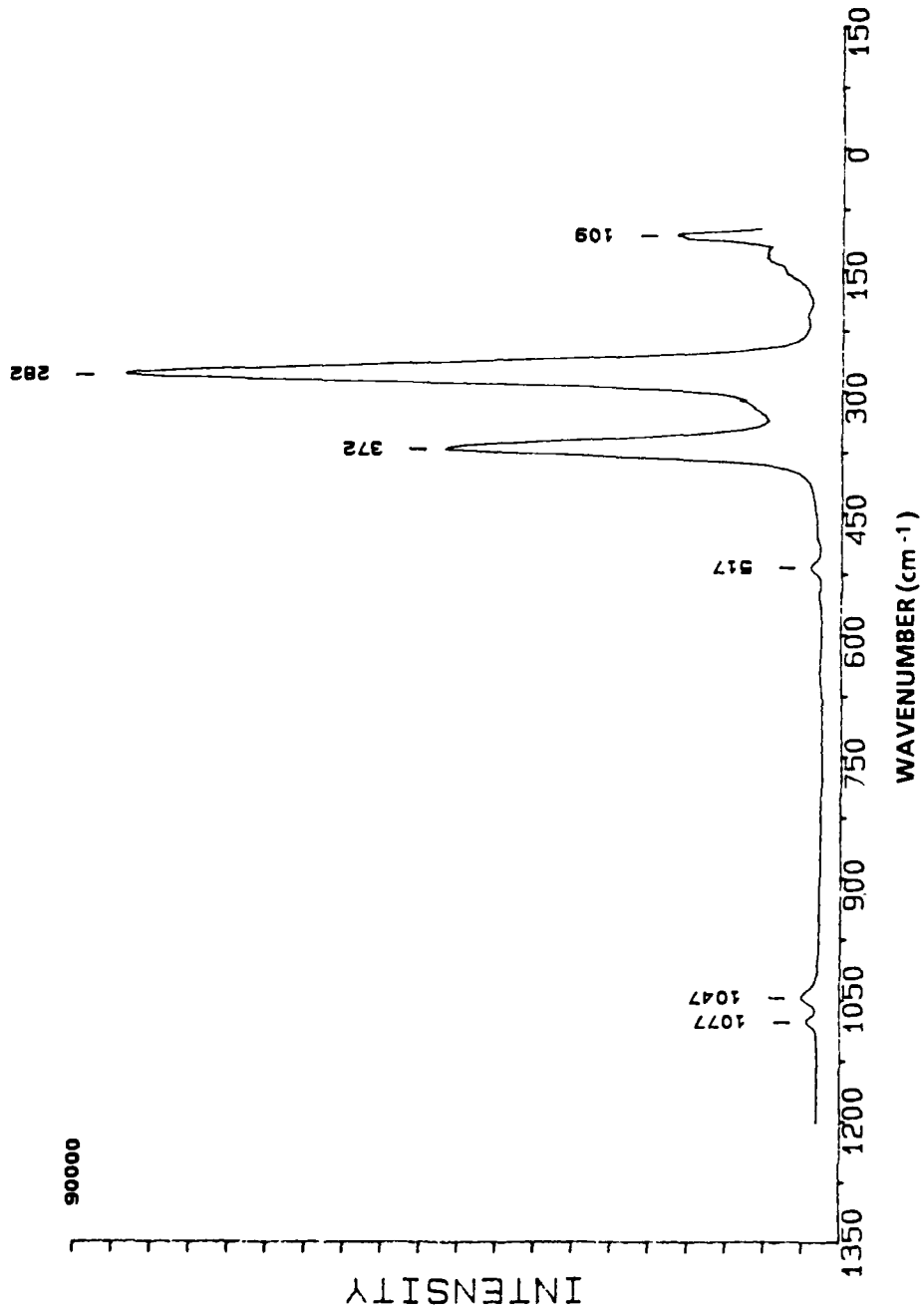


FIGURE 13. DSC CURVE AT 20°C/MIN FOR LITHIUM DITHIONITE PREPARED IN NONAQUEOUS MEDIUM

FIGURE 14. RAMAN SPECTRUM FOR $\text{Li}_2\text{S}_2\text{O}_4$ (AQUEOUS PREPARATION) 15 MIN AT 160°C

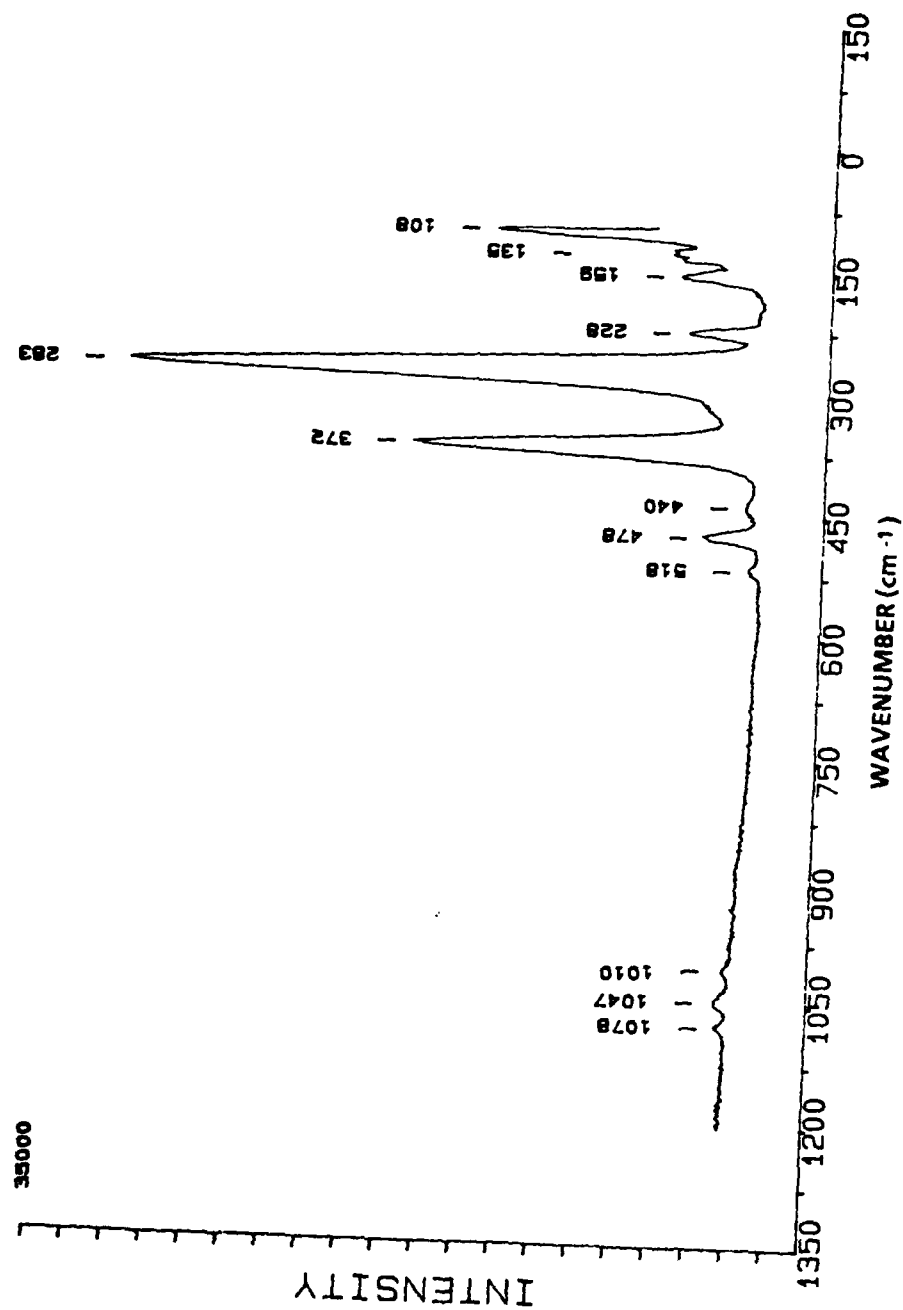
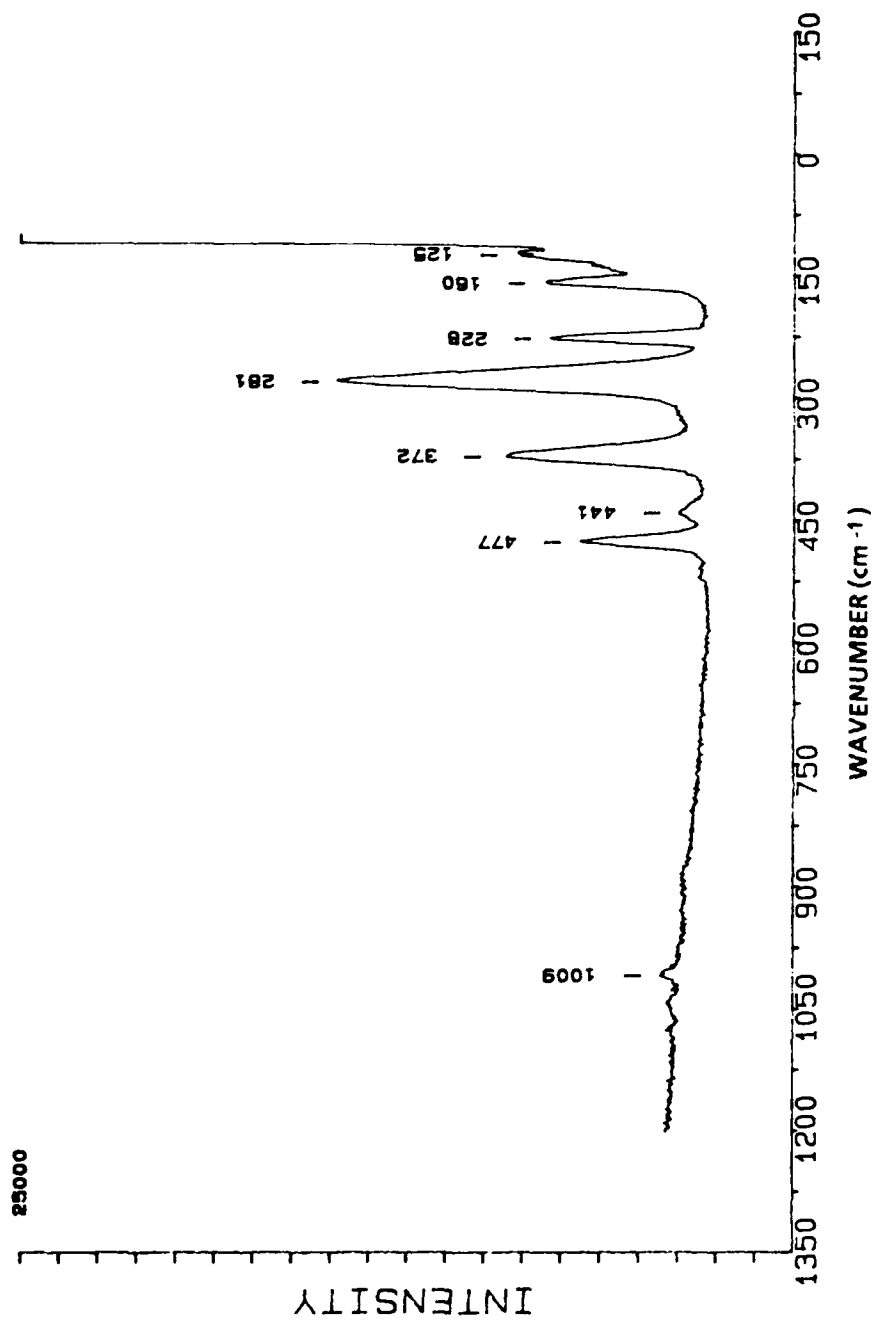


FIGURE 15. RAMAN SPECTRUM FOR $\text{Li}_2\text{S}_2\text{O}_4$ (AQUEOUS PREPARATION) 60 MIN AT 160°C

FIGURE 16. RAMAN SPECTRUM FOR $\text{Li}_2\text{S}_2\text{O}_4$ (AQUEOUS PREPARATION) 150 MIN AT 160°C

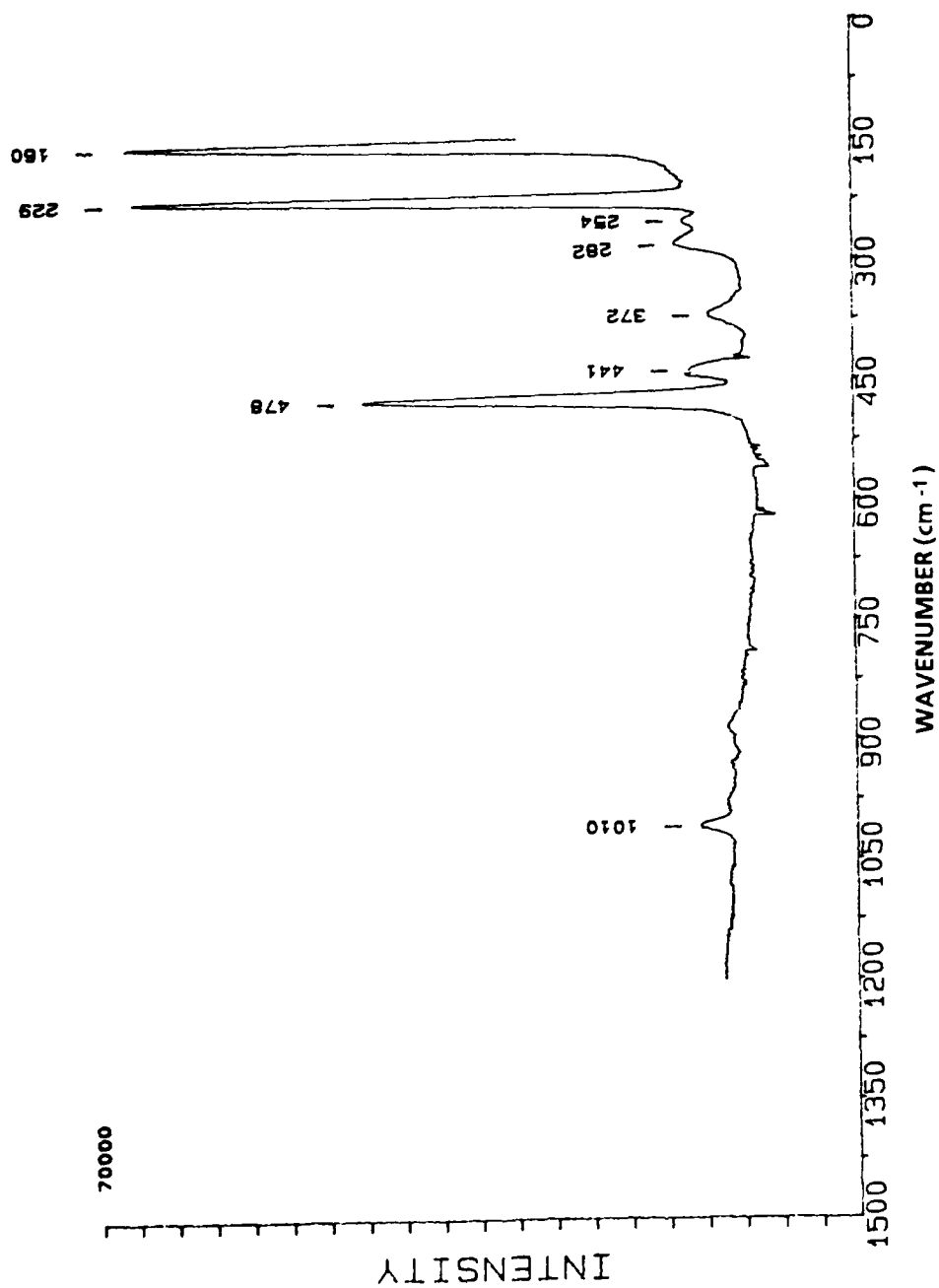
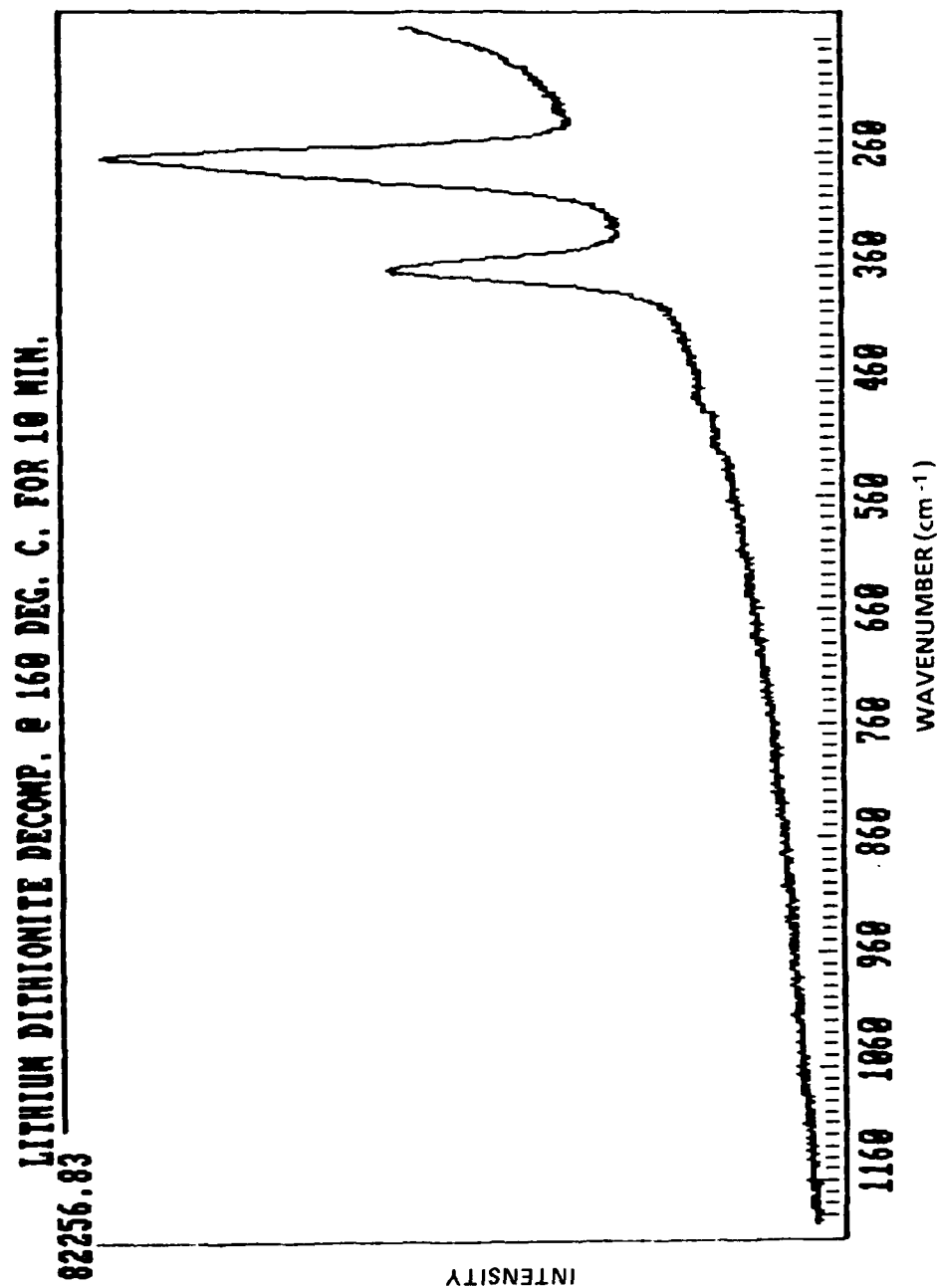
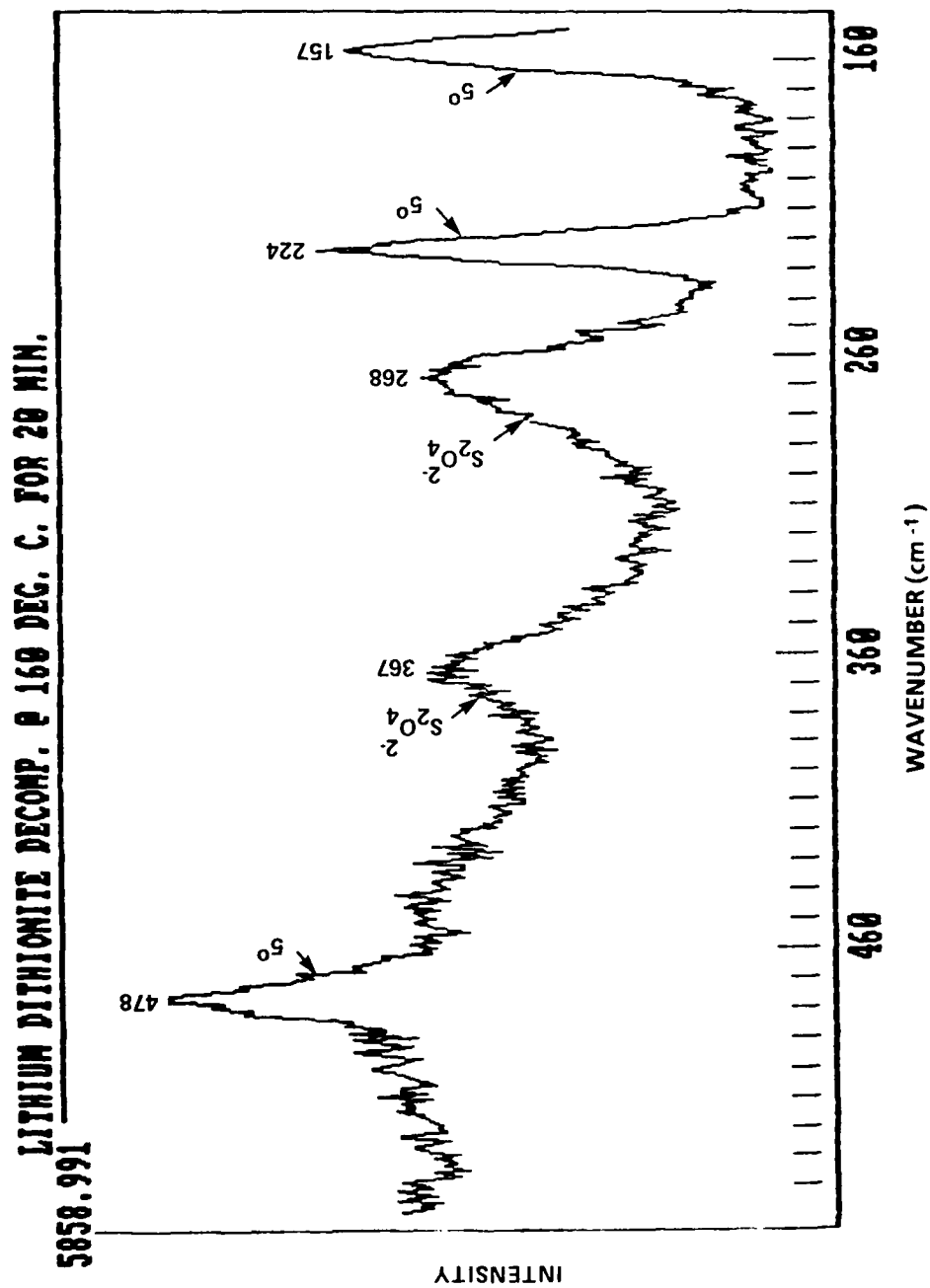


FIGURE 17. RAMAN SPECTRUM FOR $\text{Li}_2\text{S}_2\text{O}_4$ (AQUEOUS PREPARATION) 360 MIN AT 160°C

FIGURE 18. RAMAN SPECTRUM FOR $\text{Li}_2\text{S}_2\text{O}_4$ (NONAQUEOUS PREPARATION) 10 MIN AT 160°C

FIGURE 19. RAMAN SPECTRUM FOR Li₂S₂O₄ (NONAQUEOUS PREPARATION) 20 MIN AT 160°C

LITHIUM DITHIONITE DECOMP. @ 160 DEG. C. FOR 60 MIN.

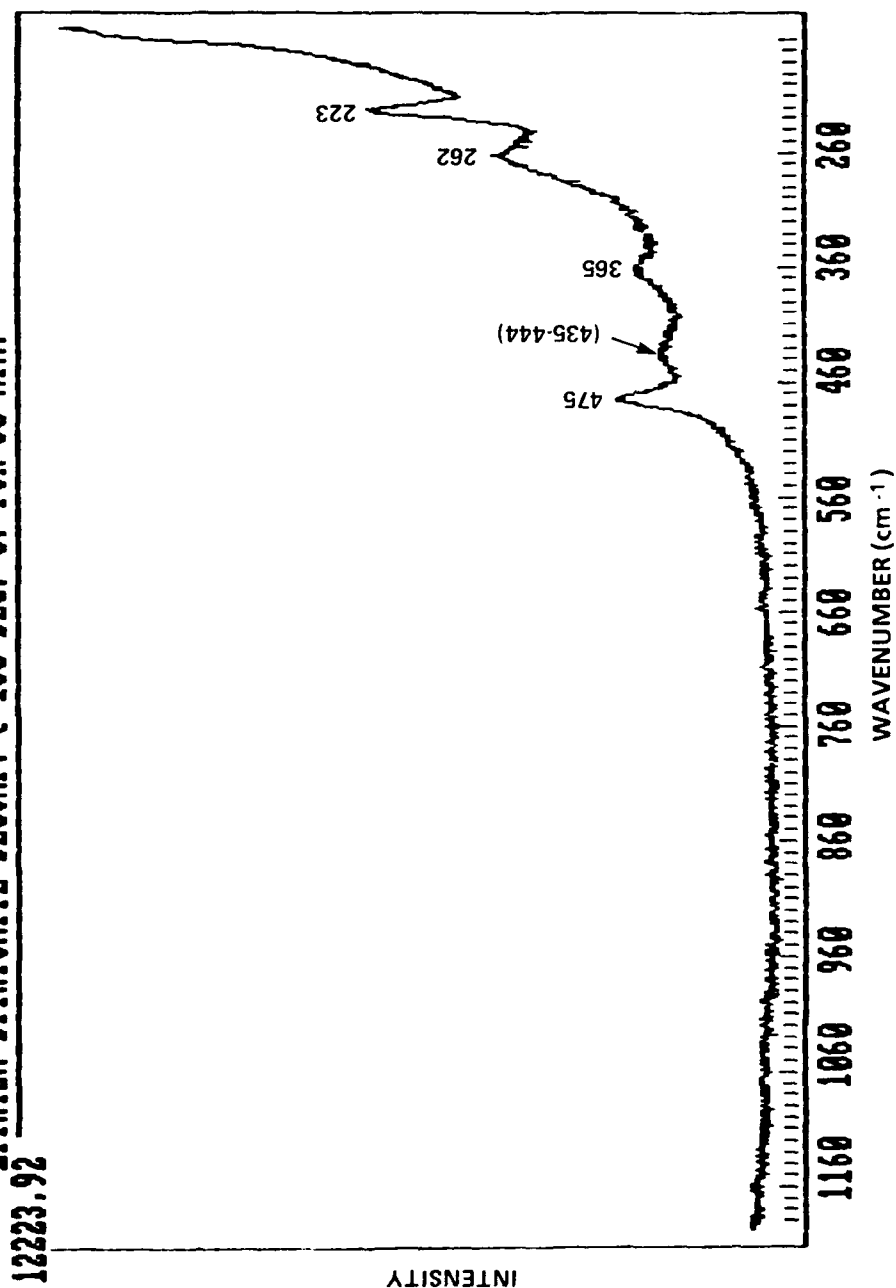


FIGURE 20. RAMAN SPECTRUM FOR $\text{Li}_2\text{S}_2\text{O}_4$ (NONAQUEOUS PREPARATION) 60 MIN AT 160°C

Raman spectroscopy is a weakly penetrating probe. It is interesting that if the partially decomposed sample in Figure 19 was ground up and another Raman spectrum taken, the relative intensity of the dithionite peaks increase significantly as shown in Figure 21. This demonstrates that most of the reaction occurred at the surface, and that the interior sample consists largely of lithium dithionite. Thus, the particle size or distribution of the sample may play a significant role in the thermal stability of the dithionite and the hazards observed in the SO_2 cell.

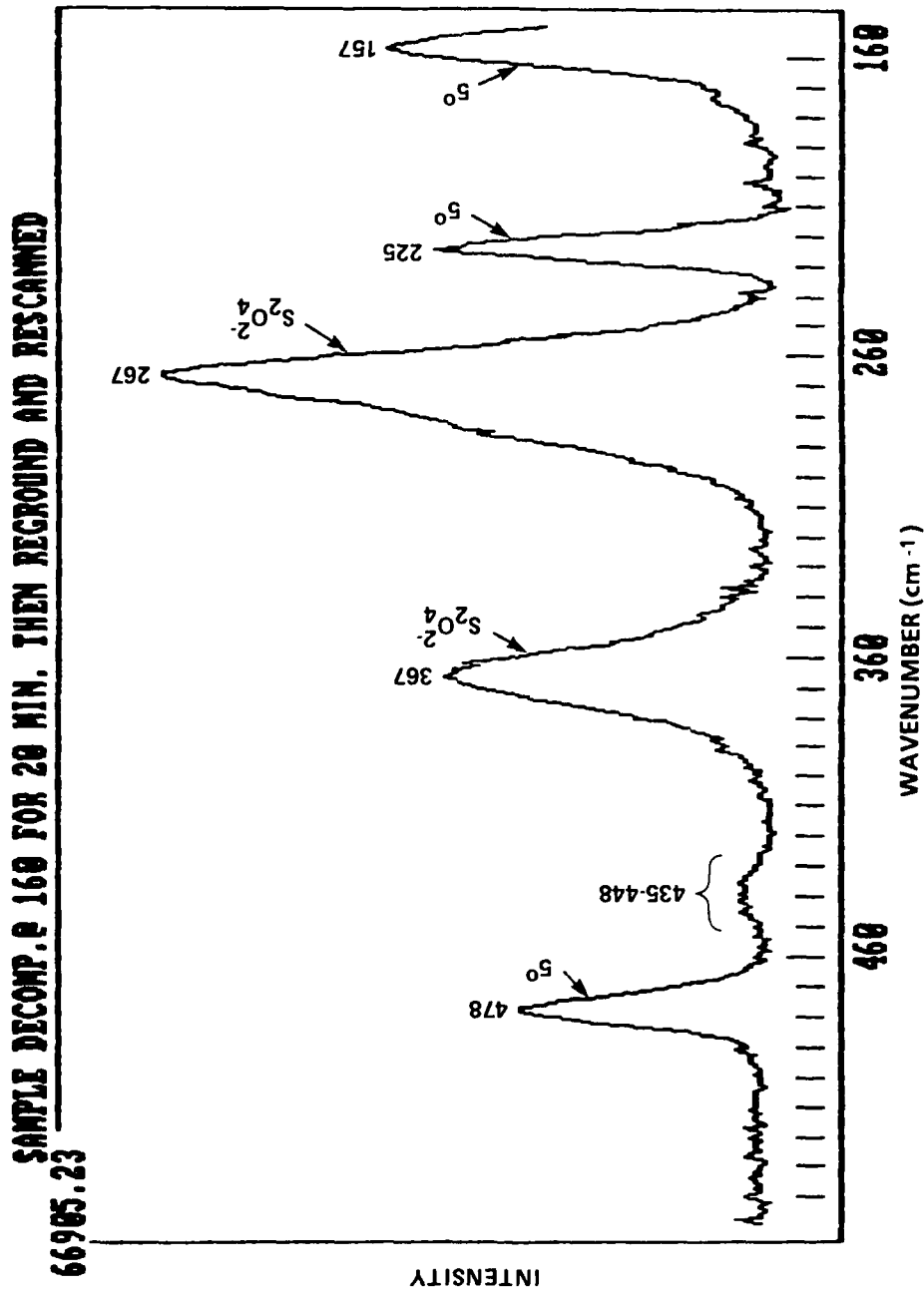


FIGURE 21. RAMAN SPECTRUM OF SAMPLE DECOMPOSED AT 160°C FOR 20 MIN (FIGURE 19), THEN REGROUND AND RESCANED

CHAPTER 4

INVESTIGATIONS OF DITHIONITE STABILIZATION

In attempting to solve the problem of the decomposition of the dithionite ion in the Li/SO_2 battery, two approaches can be envisioned. The first is an approach that has been pursued over the past few years: studying the decomposition process to access the reasons for decomposition. The long-term goal of this approach is to derive the means to inhibit battery decomposition while maintaining the structural and operational integrity of the battery.

A second approach is to modify the reactivity of the dithionite ion by coordinating it to a metal center. The metal center has the potential to impede the decomposition of the dithionite by increasing its stability through coordination, and/or modifying the reduction mechanism of SO_2 . In this approach, the dithionite ion may be rendered inert towards thermal decomposition by undergoing coordination to transition metal ions, and clues to the actual decomposition process may surface when the passivating complexes are characterized. The selection of appropriate metal centers may lead to coordination of sulfur dioxide and mediation of electron transfer through the coordinating metal center.

Iron and cobalt salts of dithionite were prepared by coprecipitation with pyridine from an aqueous solution of their chloride salts and sodium dithionite. Manganese dithionite was prepared by allowing pyridine vapor to diffuse slowly into a solution of manganese II chloride and sodium dithionite at 0°C . The crystalline compounds were dried in vacuo, and Raman spectra obtained.

The iron and cobalt complexes had no S-S or S-O Raman bands, indicating that the energy of the beam was sufficient to decompose the samples. The cobalt salt was observed to decompose spontaneously and exothermically upon standing. It is unlikely that coordination of dithionite by iron or cobalt would be a viable approach to stabilizing dithionite since its apparent rapid decomposition would likely be detrimental.

The manganese complex exhibited S-S stretching and S-O wagging modes at 275 and 369 cm^{-1} , respectively. Raman spectra of samples heated slowly in sealed capillary tubes in a regulated bath indicated decomposition begins near 110°C and is complete at 120°C after 30 minutes. Consequently, this salt was also less stable than the lithium salt, indicating manganese is not a viable candidate for enhancing battery safety.

The Raman spectra of ZnS_2O_4 (pyridine) are shown in Figures 22 and 23, respectively. Coordination of the metal has greatly reduced the O-S-O deformation as would be expected if the anion is tightly bound to the metal center (in contrast to the alkali metal salts). A notable increase occurs in the S-S stretching indicative of a much stronger S-S bond. Coordination to the zinc ion appears to have stabilized the anion to homolytic cleavage and subsequent formation of the sulfur dioxide radical anion. The salt scarcely dissolves in water, and it is clear that the susceptibility of dithionite to decomposition has been markedly altered by its coordination to zinc. Coordination stabilizes the anion towards redox decomposition since excess electron density is no longer localized on the anion but is involved in ligand-metal bonding.

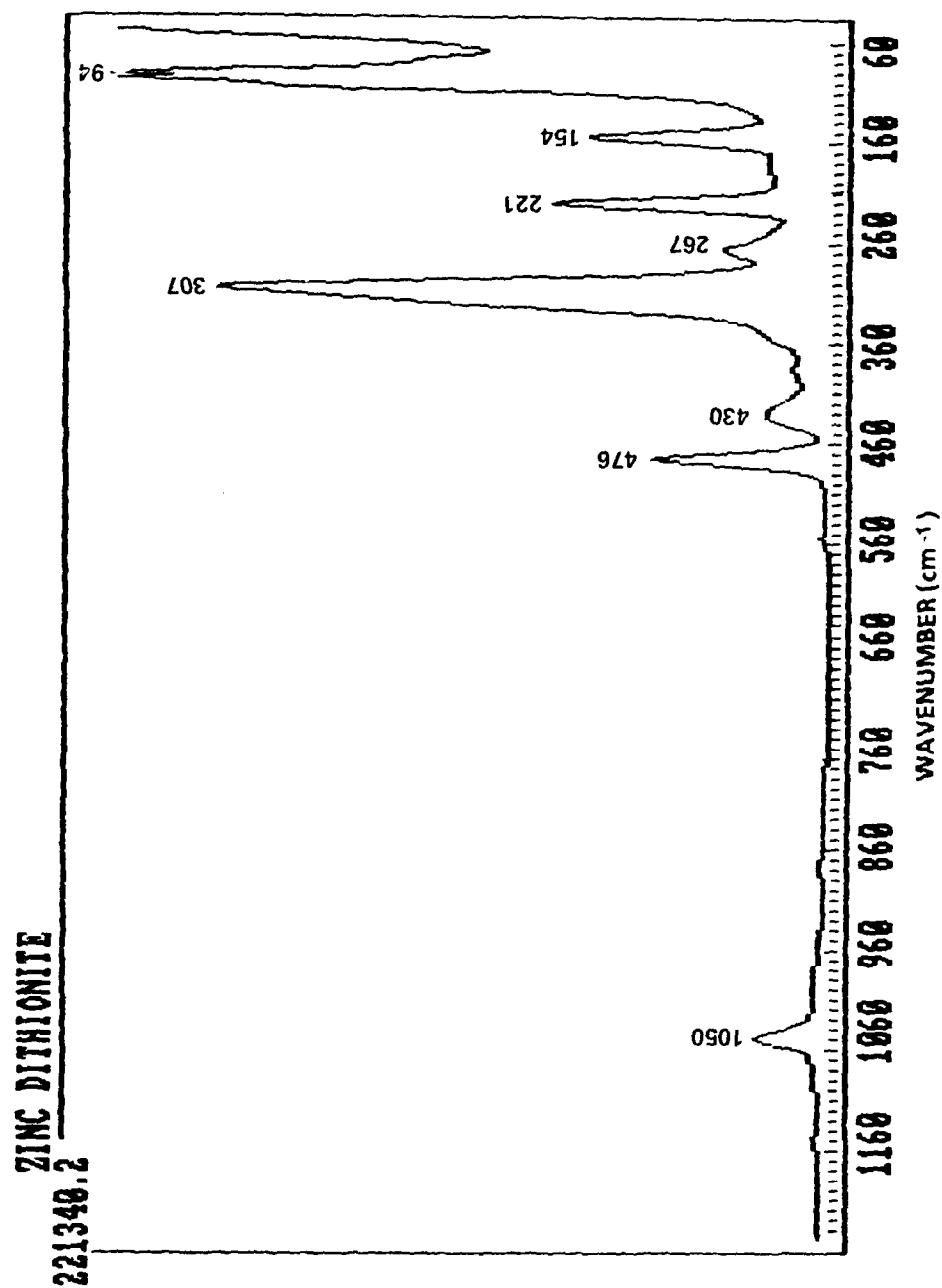


FIGURE 22. RAMAN SPECTRUM OF ZINC DITHIONITE

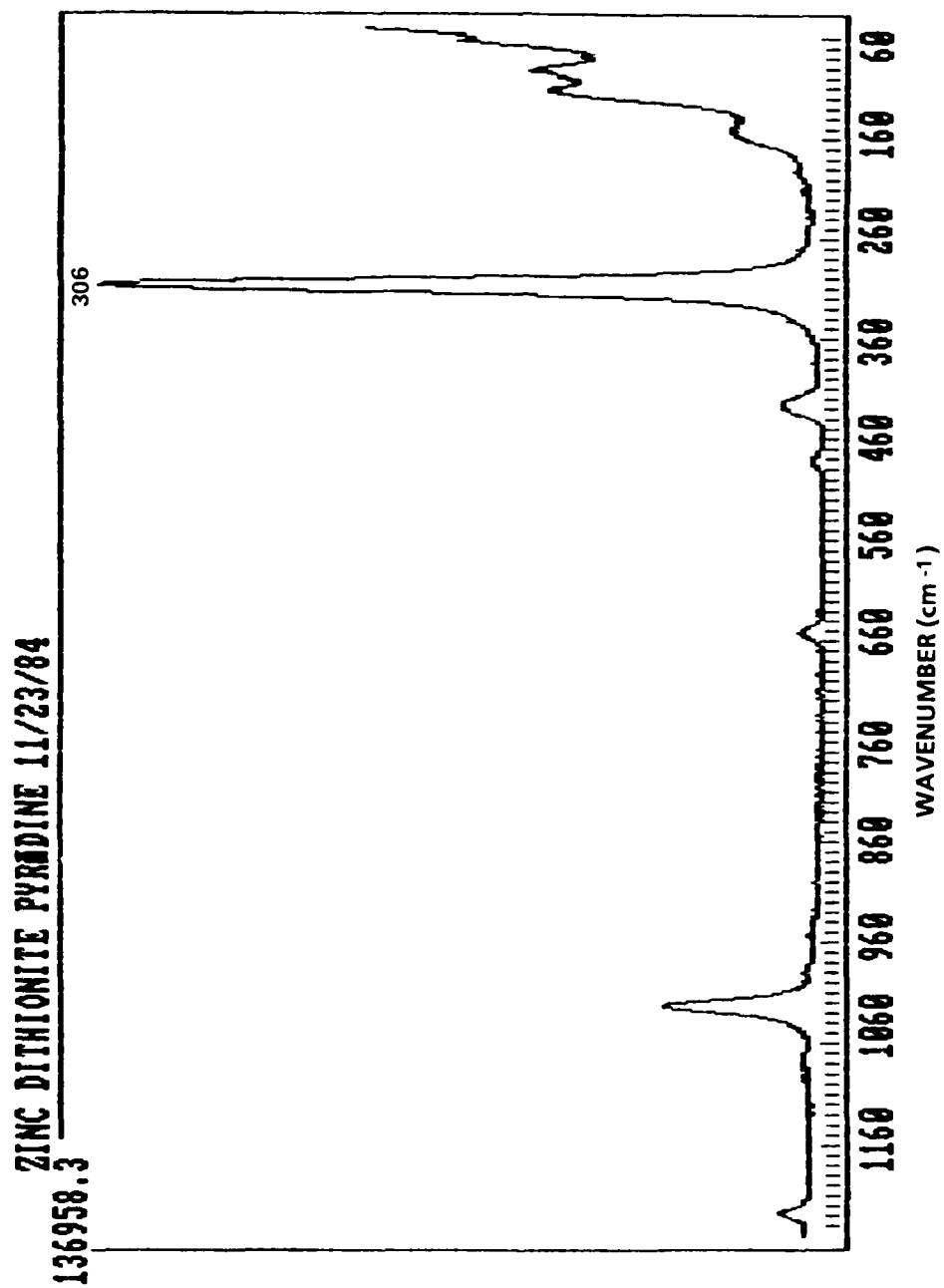


FIGURE 23. RAMAN SPECTRUM OF ZINC DITHIONITE PYRIDINE

CHAPTER 5

SUMMARY

An investigation was undertaken to improve the safety hazards associated with the use of Li-SO_2 cells. This is a relevant task since Li-SO_2 batteries are widely deployed in the Navy. Some of these safety hazards are attributed to the thermal decomposition and subsequent reactions of the lithium dithionite discharge product.

The preparation of lithium dithionite is very difficult. A variety of synthetic methods were investigated in nonaqueous media. Thermal and spectral data indicate samples prepared in aqueous and nonaqueous medium differ in stability, and may exist in two crystal configurations. This may have an important bearing on cell safety since the lithium dithionite is formed on a carbon substrate contaminated with varying concentrations of water in an otherwise nonaqueous SO_2 environment. The role that impurities play in the decomposition process still needs to be addressed. Raman data indicate that the decomposition process is dependent on the spatial geometry of the dithionite sample. ESR data on all the dithionite salts show that the anion radical concentration decreases with increasing temperature indicating that this radical concentration may not be a factor in the decomposition.

Preliminary studies indicate the dithionite anion may be stabilized by reducing its electron density through coordination with appropriate metal ions.

REFERENCES

1. Kilroy, W. P., J. Electrochemical Society, Vol. 132, 1985, p. 998.
2. Bowden, W.; Chow, L.; Demuch, P.; and Holmes, R., Journal of Electrochemical Society, Vol. 131, 1984, p. 229.
3. Kilroy, W. P., Talanta, Vol. 30, 1983, p. 419.
4. Kilroy, W. P.; Ebner, W.; Chua, D. L.; and Venkatasetty, H. V., J. Electrochem. Soc., Vol. 132, 1985, p. 274.
5. Meyer, B. and Ospina, M., Phosphorous and Sulfur, Vol. 14, 1983, p. 23.

DISTRIBUTION

	<u>Copies</u>		<u>Copies</u>
Defense Technical Information Center Cameron Station Alexandria, VA 22304-6145	12	Strategic Systems Project Office Attn: Code NSP 2721 (K. N. Boley) Code NSP 2722 (M. Meserole) Washington, DC 20360	1 1
Defense Nuclear Agency Attn: Library Washington, DC 20301	1	Naval Air Development Center Attn: Code 6012 (J. Segrest) Code 30412 (R. Schwartz) Code 3042 (L. B. Hanson) Warminster, PA 18974	1 1 1
Library of Congress Attn: Gift and Exchange Div. Washington, DC 20540	4	Naval Intelligence Support Center Attn: Code 362 (Dr. H. Ruskie) Washington, DC 20390	1
Office of Naval Research Attn: Code ONR 1113ES (R. Nowak) 800 North Quincy Street Arlington, VA 22217	1	Naval Ocean Systems Center Attn: Code 6343 (Dr. S. Szpak) Code 6343 (L. Johnson) San Diego, CA 92152	1 1
Naval Research Laboratory Attn: Code NRL 6130 (A. Simon) Chemistry Division 4555 Overlook Avenue, SW Washington, DC 20375-5000	1	U.S. Development and Readiness Command Attn: Code DRCDE-L (J. W. Crellin) 5001 Eisenhower Avenue Alexandria, VA 22333	1
Naval Air Systems Command Attn: Code NAVAIR 301C (Dr. H. Rosenwasser) Washington, DC 20361	1	Army Material and Mechanical Research Center Attn: J. J. Demarco Watertown, MA 02172	1
Space and Naval Warfare Systems Command Attn: Code PME 124-31 (A. H. Sobel) Code 01K (T. Sliwa) M. Costa Washington, DC 20360	1 1 1	USA Mobility Equipment R&D Command Attn: Code DRME-EC Electrochemical Division Fort Belvoir, VA 22060	1
Naval Sea Systems Command Attn: Code 56Z33 (E. Anderson) SEA-06H3 (H. Holter) Washington, DC 20362	1 1	Edgewood Arsenal Attn: Library Aberdeen Proving Ground Aberdeen, MD 21010	1

DISTRIBUTION (Cont.)

	<u>Copies</u>		<u>Copies</u>
U.S. Army		Naval Coastal Systems Center	
Picatinny Arsenal		Attn: Library	1
Attn: Code SAROA-FR-E-L-C		Panama City, FL 32407	
(Dr. B. Werbel)	1		
Code SARPA-ND-D-B		Naval Underwater Systems Center	
(A. E. Magistro)	1	Attn: Code SB332 (J. Model)	1
Dover, NJ 07801		P. Hallal	1
		Newport, RI 02840	
Harry Diamond Laboratories		David Taylor Research Center	
Attn: Code DELHD-DE-OP		Annapolis Laboratory	
(J. T. Nelson)	1	Annapolis, MD 21402	1
M. Templeman	1		
Department of Army Material		Air Force Wright Aeronautical Labs	
Chief, Power Supply Branch		Aero Propulsion Lab., POOC	
2800 Powder Mill Road		Attn: Code AFAPL/POE-1	
Adelphi, MD 20783		(W. S. Bishop)	1
		Code AFWAL-POOS-2	
HQ, Department of Transportation		(R. Marsh)	1
Attn: Code GEOE-3/61 (R. Potter)	1	Wright-Patterson AFB, OH 45433	
U.S. Coast Guard			
Ocean Engineering Division		Air Force Rocket Propulsion Lab	
Washington, DC 20590		Attn: Code MKPA	
		(Lt. D. Ferguson)	1
NASA Headquarters		Edwards Air Force Base, CA 93523	
Attn: Dr. J. H. Ambrus	1		
Washington, DC 20546		HQ, Air Force Special	
		Communications Center	
NASA Lewis Research Center		Attn: Library	1
Attn: Code MS309-1		USAFSS	
(J. S. Fordyce)	1	San Antonio, TX 78243	
M. Reid	1		
2100 Brookpark Road		Office of Chief of R&D	
Cleveland, OH 44135		Department of the Army	
		Attn: Dr. S. J. Magram	1
Naval Weapons Center		Energy Conversion Branch	
Attn: Code 38 (Dr. E. Royce)	1	Room 410, Highland Building	
Code 3852 (Dr. M. Miles)	1	Washington, DC 20315	
D. Rosenlof	1		
Code 3626 (W. Haight)	1	U.S. Army Research Office	
China Lake, CA 93555		Attn: B. F. Spielvogel	1
		G. Neece	1
Naval Weapons Support Center		P. O. Box 12211	
Attn: Code 305 (M. Robertson)	1	Research Triangle Park, NC 27709	
D. Mains	1		
Code 3054 (S. Shuler)	1		
W. Johnson	1		
R. Haag	1		
Electrochemical Power Sources Div.			
Crane, IN 47522			

DISTRIBUTION (Cont.)

	<u>Copies</u>		<u>Copies</u>
NASA Scientific and Technical Information Facility		NASA Johnson Space Center	
Attn: Library	1	Attn: EPS (Bob Bragg)	1
Code 711.2 (T. Yi)	1	Houston, TX 77058	
P. O. Box 33		Office of Naval Technology	
College Park, MD 20740		Attn: ONT Code 23	
		(A. J. Faulstich)	1
National Bureau of Standards		ONT Code 23	
Metallurgy Division		(D. Houser)	1
Inorganic Materials Division		ONT Code 235	
Washington, DC 20234	1	(W. Ching)	1
		800 North Quincy Street	
U.S. Army Electronics Command		Arlington, VA 22217	
Attn: Code DRSEL-TL-P		Central Intelligence Agency	
(A. J. Legath)	1	Attn: OTS (C. Sculla)	1
Code DRSEL-TL-PD		T. Mahy	1
(E. Brooks)	1	Washington, DC 20505	
G. DiMasi	1	HQ, U.S. Marine Corps	
Dr. W. K. Behl	1	Attn: LMA-3 (LTCOL W. Lowe)	1
Code DELET-PR		Washington, DC 20380	
(Dr. Sol Gilman)	1	Missile Systems Safety	
C. Berger	1	Attn: ESMC/SEM (Kenn Hill)	1
M. Salomon	1	Patrick AFB, FL 32925	
E. Reiss	1	California Institute of Technology	
J. Perry	1	Attn: Library	1
R. Mohlenhoff	1	H. Frank	1
M. Brundage	1	S. Yen	1
D. Barker	1	G. Halpert	1
Fort Monmouth, NJ 07703		S. Dawson	1
Scientific Advisor		D. Shen	1
Attn: Code AX	1	A. Attia	1
Commandant of the Marines		C. Jaeger	1
Washington, DC 20380		S. Surampuda	1
Air Force of Scientific Research		Jet Propulsion Laboratory	
Attn: Dir. of Chemical Science	1	4800 Oak Grove Drive	
1400 Wilson Boulevard		Pasadena, CA 91109	
Arlington, VA 22209		Johns Hopkins Applied Physics Lab	
Frank J. Seiler Research Lab, AFSC		Attn: Library	1
USAF Academy, CO 80840	1	M. Uy	1
Department of National Defense		Johns Hopkins Road	
Attn: Library	1	Laurel, MD 20707	
W. Adams	1	University of Tennessee	
G. Donaldson	1	Attn: G. Mamantov	1
J. Lackner	1	Department of Chemistry	
Defense Rsch Establishment Ottawa		Knoxville, TN 37916	
Ottawa, Ontario K1A 0Z4 Canada			

DISTRIBUTION (Cont.)

	<u>Copies</u>		<u>Copies</u>
University of Wisconsin-Milwaukee		Ministere de la defense nationale	
Attn: Dr. D. Bennett	1	Attn: Dr. W. Adams	1
Chemistry Department		Dr. G. Donaldson	1
3210 North Cramer Street		Centre de recherches pour la defense	
Milwaukee, WI 53201		Ottawa, Ontario K1A 0Z4 Canada	
 State University of New York		 Chemtech Systems, Inc.	
Attn: Dr. R. A. Osteryoung	1	Attn: Dr. M. L. Gopikanth	1
Department of Chemistry		P. O. Box 1067	
Buffalo, NY 14214		Burlington, MA 01803	
 Argonne National Laboratory		 Power Information Center	
Attn: Dr. E. C. Gay	1	CSR, Inc.	
Dr. D. Vissars	1	1400 Eye Street, N.W.	
Dr. J. Rajan	1	Suite 600	
9700 South Cass Avenue		Washington, DC 20005	1
Argonne, IL 60439		 Internal Distribution:	
 Sandia Laboratories		E231	2
Attn: Mail Services Sect. 3154-3		E232	15
(Sam Levy)	1	E35	1
J. Searcy	1	R33 (W. P. Kilroy)	30
W. Cieslak	1		
N. Magnani	1		
P. O. Box 5800			
Albuquerque, NM 87715			